doi:10.1016/j.jmb.2004.05.031 *J. Mol. Biol.* (2004) **341**, 839–852

JMB

Available online at www.sciencedirect.com

SCIENCE DIRECT®

ELSEVIER

The Crystal Structure of ZapA and its Modulation of FtsZ Polymerisation

Harry H. Low[1]*, Martin C. Moncrieffe[2] and Jan Löwe[1]

[1]*MRC Laboratory of Molecular Biology, Hills Road, Cambridge CB2 2QH, UK*

[2]*Department of Biochemistry University of Cambridge 80 Tennis Court Road Old Addenbrookes Site Cambridge CB2 1GA, UK*

**Corresponding author*

FtsZ is part of a mid-cell cytokinetic structure termed the Z-ring that recruits a hierarchy of fission related proteins early in the bacterial cell cycle. The widely conserved ZapA has been shown to interact with FtsZ, to drive its polymerisation and to promote FtsZ filament bundling thereby contributing to the spatio-temporal tuning of the Z-ring. Here, we show the crystal structure of ZapA (11.6 kDa) from *Pseudomonas aeruginosa* at 2.8 Å resolution. The electron density reveals two dimers associating *via* an extensive C-terminal coiled-coil protrusion to form an elongated anti-parallel tetramer. In solution, ZapA exists in a dimer–tetramer equilibrium that is strongly correlated with concentration. An increase in concentration promotes formation of the higher oligomeric state. The dimer is postulated to be the predominant physiological species although the tetramer could become significant if, as FtsZ is integrated into the Z-ring and is cross-linked, the local concentration of the dimer becomes sufficiently high. We also show that ZapA binds FtsZ with an approximate 1 : 1 molar stoichiometry and that this interaction provokes dramatic FtsZ polymerisation and inter-filament association as well as yielding filaments, single or bundled, more stable and resistant to collapse. Whilst *in vitro* dynamics of FtsZ are well characterised, its *in vivo* arrangement within the ultra-structural architecture of the Z-ring is yet to be determined despite being fundamental to cell division. The ZapA dimer has single 2-fold symmetry whilst the bipolar tetramer displays triple 2-fold symmetry. Given the symmetry of these ZapA oligomers and the polar nature of FtsZ filaments, the structure of ZapA carries novel implications for the inherent architecture of the Z-ring *in vivo*.

Keywords: Bacterial cell division; Z-ring; X-ray

Introduction

The discovery that the FtsZ GTPase formed a circumferential cytokinetic scaffold at the mid-cell yielded a potential molecular mechanism for bacterial cell division and its regulation.[1] Subsequent immunofluorescence analysis demonstrated the prominence of this structure early in the cell cycle,[2,3] whilst GFP confirmed the three-dimensional nature of this "Z-ring".[4,5] Visualisation of FtsZ at atomic resolution[6] revealed a structure with strong homology to eukaryotic tubulin[7,8] that naturally alluded to a prokaryotic origin for this key eukaryotic structural element. Further similarity between these two evolutionarily distant domains emerged amongst other components of the prokaryotic cytoskeletal machinery, for example between MreB and eukaryotic actin,[9,10] and more recently Crescentin and eukaryotic intermediate filaments,[11] which reinforced the theory that these are examples of true homology rather than convergence. FtsZ is remarkably conserved amongst the Eubacteria and Archaea with those lacking a Z-ring being an exception.[12,13] Its existence has also been shown in chloroplasts[14] and more recently in mitochondria.[15,16]

It is thought that the precise selection of the division site, usually at the mid-cell, is controlled by localisation of the Z-ring through several mechanisms of which the Min system is the best characterised.[17,18] A hierarchy of cytoplasmic and membrane proteins, both intrinsic and extrinsic, are subsequently recruited to the Z-ring and have

Abbreviations used: MAP, microtubule-associated protein.

E-mail address of the corresponding author: hlow@mrc-lmb.cam.ac.uk

diverse roles[18–20] that include anchoring the ring to the cell membrane, invagination and constriction, septum formation and peptidoglycan synthesis to yield two separate daughter cells. *In vitro*, FtsZ is extremely versatile, forming protofilaments, thick filaments, sheets,[21,22] helical tubes[23,24] and asters.[25] This ability to form an array of dynamic polymers is dependent on GTP hydrolysis[26,27] and strong inter-molecular longitudinal contacts. During polymerisation, the FtsZ T7 loop extends into the nucleotide-binding active site of a neighbouring subunit and likely mediates the polymerisation-dependent GTPase activation mechanism.[22,28] Weaker lateral contacts are also involved in defining polymer character,[29] perhaps through the S3 strand[21,22] or the N-terminal helix, but these are much less well understood. Despite such *in vitro* knowledge, the inherent morphology of the Z-ring *in vivo* still remains obscured.

There are a host of accessory proteins involved in regulating FtsZ polymerisation dynamics and which together contribute to the exquisite spatio-temporal tuning of the Z-ring. Acting negatively, the Min system involves accumulation of division inhibitors MinC and MinD at the cell poles *via* non-universally conserved mechanisms that are dependent on topological specificity factors, namely MinE in *Escherichia coli*[30,31] or DivIVA in *Bacillus subtilis*.[32,33] EzrA is another known FtsZ destabilising agent whose deletion in *B. subtilis* both provokes the formation of multiple Z-rings at polar and medial locations, and decreases the critical concentration of FtsZ required for ring formation.[34] Also acting negatively, the SOS cell division inhibitor SulA in *E. coli* binds directly to FtsZ,[35–37] prevents Z-ring assembly and consequently inhibits cell division.

In contrast, there are antagonistic proteins that promote FtsZ stability and drive its intra-cellular equilibrium towards filament formation. FtsA is essential for the recruitment of division components *via* direct interaction with the Z-ring early in the cell cycle.[38] In addition, it is required for Z-ring assembly and stabilisation,[39] perhaps through membrane association, whilst its ability to dimerise[40] suggests a possible secondary role in FtsZ cross-linking. In *E. coli*, ZipA is as important as FtsA in downstream recruitment[41] and has also been shown to interact directly with FtsZ.[42] Over-expression of this membrane-associated protein abolishes cell division and suppresses the classic temperature-sensitive *ftsZ84* mutant through its ability to bundle and stabilise FtsZ protofilaments.[43,44] Although ZipA may exhibit homology to eukaryotic microtubule-associated proteins (MAPs)[44] its existence is restricted within the γ-proteobacteria.

Recently, another FtsZ stabilising agent has been discovered with broad conservation amongst bacterial species including *E. coli*. The *Z*-ring associated protein ZapA has been shown to interact with FtsZ and to direct the formation of heavily bundled and branched filamentous networks *in vitro*.[45] Light-scattering assays demonstrate ZapA is capable of driving FtsZ polymerisation independently of nucleotide although polymerisation is shown to be highly accentuated in the presence of GTP. Electron microscopy reveals either filament bundling reminiscent of ZipA–FtsZ synergy or the promotion of ~25 nm diameter mini rings when associated with either GTP or GDP, respectively.

Despite the extensive conservation of ZapA, Z-ring formation in null mutants is indistinguishable from wild-type with no significant division defect. However, ZapA deletion becomes lethal when combined as a double mutant with either EzrA or DivIVA, or in cells with reduced FtsZ levels.[45] ZapA seemingly differs from other known FtsZ stabilising elements, such as FtsA and ZipA, as its deletion yields no obvious abnormality and is non-lethal. However, these molecules are likely indispensable as a result of the downstream division events they orchestrate rather than their stabilising role. Thus, ZapA seems unique in its specific dedication to the modulation of FtsZ polymerisation and regulation of Z-ring dynamics. Here, we have used X-ray crystallography to elucidate the structure of this 11.6 kDa protein and biochemical techniques to further characterise its interaction with FtsZ.

Results

ZapA oligomerisation

The full-length *Pseudomonas aeruginosa* ZapA, comprising 104 amino acid residues, was crystallised and solved to 2.8 Å resolution in space group $P4_12_12$. The electron density reveals two ZapA dimers associating *via* an extensive C-terminal coiled coil protrusion to form an anti-parallel tetramer. This initially appears contrary to previous expectations, as ZapA from *B. subtilis* was predicted to be dimeric.[45] The integrity of the tetramer was confirmed in solution by size-exclusion chromatography (Figure 1G) and electro-spray mass spectrometry (Figure 1F). For the chromatography we used a Biosep SEC S3000 column calibrated with five standards ranging from 29 kDa to 440 kDa. ZapA at 10 mg/ml eluted as a single species with $K_{va} = 0.52$ which yields a calculated molecular mass of 66.6 kDa (K_{va} of the theoretical 50.5 kDa tetramer = 0.55). For the mass spectrometry, acceleration voltages and vacuum pressures in the source and ion transfer stages of the mass spectrometer were carefully adjusted for sufficient desolvation of macromolecular ions while maintaining non-covalent interactions during collisional cooling. There were no unassigned peaks in the ESI mass spectra. Experimental masses (Da): monomer 12,492.08 ± 0.21 (poly-His ZapA minus N-terminal methionine: calculated 12,490); dimer 24,991.86 ± 12.88; tetramer 50,012.28 ± 21.71. More specifically, sedimentation velocity analytical ultracentrifugation shows ZapA is not exclusively a tetramer in

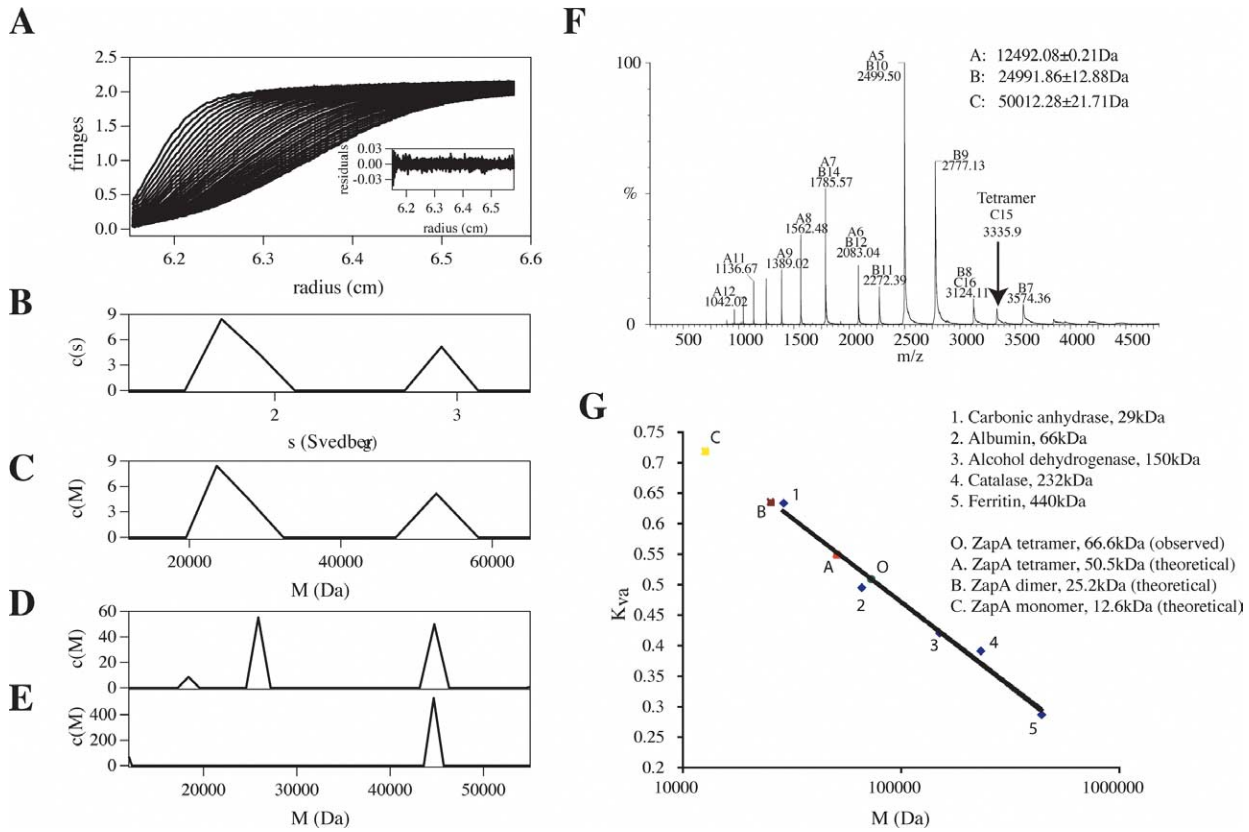

Figure 1. ZapA exists in a dimer–tetramer equilibrium dependant on concentration. A–E, Sedimentation velocity analytical ultracentrifugation of ZapA over a range of concentrations. Successive sedimentation scans at three minute intervals (A), sedimentation coefficients (B) and molecular mass (C) of ZapA at 0.6 mg/ml ($A_{280} = 0.2$). ZapA is predominantly dimeric (MW = 23,612 Da) although some tetramer (MW = 52,619 Da) exists at this concentration. D, Increasing ZapA concentration (2.5 mg/ml ($A_{280} = 0.75$)) promotes inter-dimer association. An approximately equal mixture of dimer and tetramer exists. E, At 10 mg/ml, ZapA is entirely tetrameric (MW = 44,672 Da). F, Electro spray mass spectrometry of ZapA injected at 25 μM. Charge series for monomer, dimer and tetramer are observed. G, ZapA is a tetramer (O) running as a single peak when gel filtered at 10 mg/ml, $K_{va} = 0.52$. Note positions of theoretical monomer (C), dimer (B) and tetramer (A) ($K_{va} = 0.55$).

solution (Figure 1A–E). At high concentration (10 mg/ml), ZapA sediments as a single tetrameric species with a calculated molecular mass of 44,671.9 kDa (theoretical = 50.5 kDa) (Figure 1E). When the concentration is decreased to 0.6 mg/ml ($A_{280} = 0.2$), the predominant oligomeric species is now dimeric (MW = 23,612 Da) although some tetramer persists (MW = 52,619 Da) (Figure 1C). At a mid-range concentration of 2.5 mg/ml ($A_{280} = 0.75$), the sedimentation centrifugation shows a clear mixture of both dimer and tetramer (Figure 1D). Therefore, the oligomeric state of ZapA assumes a dimer–tetramer equilibrium that is strongly correlated to concentration. Increasing concentration drives the equilibrium towards a tetrameric state whilst a decrease favours dissociation into dimer.

The crystal structure of ZapA

The asymmetric unit comprises two dimerised subunits with ordered amino acid residues 6–96 and 5–95 (Figure 2B; subunits A and B, respectively). In the model, a 180° crystallographic rotation of dimer AB perpendicular to its long axis yields the complete tetramer with general triple 2-fold symmetry (point group 222) (Figure 2B). This symmetry is not absolute as a consequence of crystal packing and flexibility in the molecule. Crystallographic data and refinement statistics are summarised in Tables 1 and 2.

The monomer consists of a short N-terminal double-stranded anti parallel β-sheet (S1, residues 7–11 and S2, residues 14–18) conjoined with a left-handed α-turn. Helix H1 (residues 24–45) lies adjacent, running parallel with the sheet and opening onto the dominant architectural feature, helix H2. This C-terminal helix protrudes centrally for 45 or 46 amino acid residues (depending on the subunit) along the longitudinal axis of the molecule initiating at residue 50 (Figures 2A, C and 3). The dimer interface between subunit A and B comprises 13% of the monomer surface (half 3038 Å^2 of 12087 Å^2) whilst the tetramer interface between dimers AB and CD covers 8% of each dimer surface (half 3391 Å^2 of 20799 Å^2). Thus, the proportion of the dimer surface dedicated exclusively to forming the tetramer interface is not

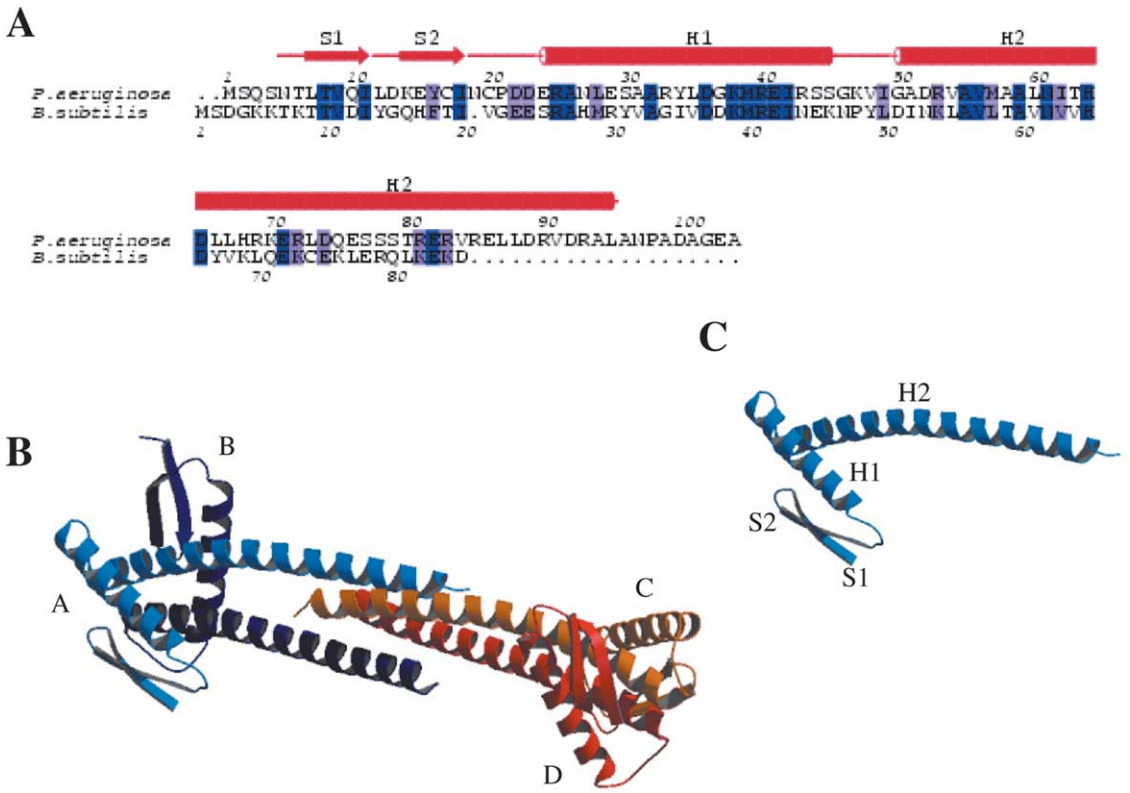

Figure 2. A, Sequence alignment of ZapA from *P. aeruginosa* with *B. subtilis*. Observed secondary structural elements are shown according to DSSP output.[68] Identical residues are dark blue; similar residues are light blue (according to GAP; GCG Wisconsin package). Sequence similarity and identity are 39.8% and 25.3%, respectively, between the two proteins. B, Ribbon diagram of the ZapA tetramer; dimer AB made by non-crystallographic symmetry and dimer CD by crystallographic symmetry. (A and C comprise amino acid residues 6–96; B and D, 5–95) (prepared in MOLSCRIPT). C, Ribbon diagram of the ZapA monomer.

much smaller than the interface utilised by two monomers to complex, reflecting a compact and intimately bound tetramer approximately 100 Å long in total. Contact between the subunits A and B (and equally C and D) is most significant towards the N termini of the H2 helices as a consequence of a conserved and opposing core of predominantly hydrophobic amino acid residues (Val54-Leu67) (Figure 3). Dimerisation is further reinforced by interaction from, for example, the N termini of both helix H1 and strand S2 of subunit A against the neighbouring H2 helix of subunit B. The tetramerisation domain, or inter-dimer overlap along the axis of the H2 α-helix, is extensive corresponding to approximately five turns or 27 Å and up to 18 residues depending on the subunit (Figure 3). The inner faces of these four overlapping helices form an elongated central tunnel dominated by side-chain protrusions from hydrophobic amino acid residues (Val84, Leu87/88, Val91 and Leu95). Surrounding these hydrophobic strips are hydrophilic residues whose side-chains tend to interdigitate as a consequence of slight staggering between dimers AB and CD. It is

Table 1. Crystallographic data

Pseudomonas aeruginosa ZapA–selenomethionine substituted
Space group $P4_12_12$, $a = b = 105.2$ Å, $c = 36.0$ Å, two molecules/ASU

Crystal	λ (Å)	res. (Å)	$I/\sigma I$[a]	R_m (%)[b]	Multipl.[c]	Compl. (%)[d]
PEAK	0.9802	2.7	23.8(6.6)	0.071(0.281)	11.9	99.7(98.6)
INFL	0.9806	2.7	23.1(6.4)	0.069(0.286)	12.0	99.5(97.5)
HREM	0.9700	2.7	44.7(24.8)	0.039(0.081)	12.0	99.3(99.1)

[a] Signal to noise ratio of merged intensities, in parentheses for the highest resolution shell.
[b] R_m:$\sum_h \sum_i |I(h,i) - I(h)| / \sum_h \sum_i I(h,i)$ where $I(h,i)$ are symmetry-related intensities and $I(h)$ is the mean intensity of the reflection with unique index h. In parentheses for the highest resolution bin.
[c] Multiplicity for unique reflections.
[d] Completeness for unique reflections, anomalous completeness is identical because inverse beam geometry was used. In parentheses for the highest resolution bin. Correlation coefficients of anomalous differences at different wavelengths for the MAD experiment: PEAK *versus* INFL: 0.72, PEAK *versus* HREM: 0.88, *versus* HREM: 0.71.

Table 2. Refinement statistics

Model	Two non-crystallographically related chains, A + B A: residues 6–96 B: residues 5–95 12 water molecules
Diffraction data	2.8 Å, all data
R-factor, *R*-free[a]	0.240(0.329), 0.289(0.375)
B average/bonded (Å^2)[b]	53.7, 4.049
Geometry bonds/angles[c]	0.007 Å, 1.199°
Restrained NCS	No restraints used
Ramachandran (%)[d]	94.1/0.0
PDB ID	1w2e

[a] Five percent of reflections were randomly selected for determination of the free *R*-factor, prior to any refinement. High-resolution bin in parentheses.
[b] Temperature factors averaged for all atoms and RMS deviation of temperature factors between bonded atoms.
[c] RMS deviations form ideal geometry for bond lengths and restraint angles.
[d] Percentage of residues in the "most favoured region" of the Ramachandran plot and percentage of outliers.

difficult to ascertain whether such considerable and highly specific overlap of the H2 α-helices is due to evolutionary design and *in vivo* function, or is simply the extraneous consequence of coiled-coil interaction at high concentration. It is postulated that the predominant physiological species of ZapA is likely to be dimeric. However, as ZapA cross-links FtsZ polymer during Z-ring assembly, the local concentration of ZapA may be sufficient to provoke tetramer formation. Such ZapA oligomerisation would enhance the ability of this molecule to bind, cross-link and stabilise the Z-ring scaffold.

ZapA–FtsZ pelleting assays

Pelleting assays were designed both to determine quantitatively the stoichiometric relationship between ZapA and FtsZ and to probe the effect their interaction has on filament stability. When the FtsZ concentration is held constant against decreasing concentrations of ZapA and *vice versa* from a three times excess, only when the molar ratio of both proteins is matched does the FtsZ and ZapA predominantly localise in the pellet (Figure 4A). At non-symmetrical protein concentrations, residual FtsZ or ZapA not directly involved in filament formation appears in the supernatant after centrifugation. This result infers a molecular binding ratio close to 1 : 1 between FtsZ and ZapA, which is in direct accordance with a light-scattering assay undertaken in the original *B. subtilis* ZapA study.[45]

To quantify and reinforce this, if the level of FtsZ (mg/ml) is held constant against increasing levels of ZapA up to a five times excess, unbound ZapA should collect quantitatively and proportionately in the supernatant (Figure 4B). At a concentration of 1 mg/ml for both proteins, if these molecules do associate with equal stoichiometry it is expected (given the molecular mass of *P. aeruginosa* FtsZ

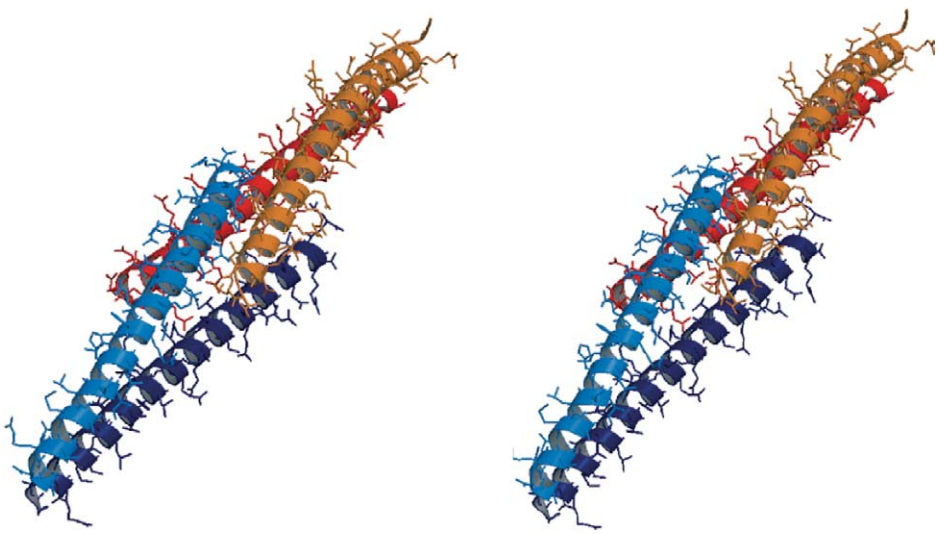

Figure 3. Stereo image showing the conformation of the four H2 helices in a ZapA tetramer with their side-chains exposed. The tetramerisation domain is formed by extensive overlap between the C termini of the H2 helices. This region is characterised by a central hydrophobic core and surrounding hydrophilic amino acid residues with inter-digitating side-chains. In contrast, the dimerisation domain is located towards the opposite ends of the H2 helices with inter-helix proximity and contact increasing towards the N termini.

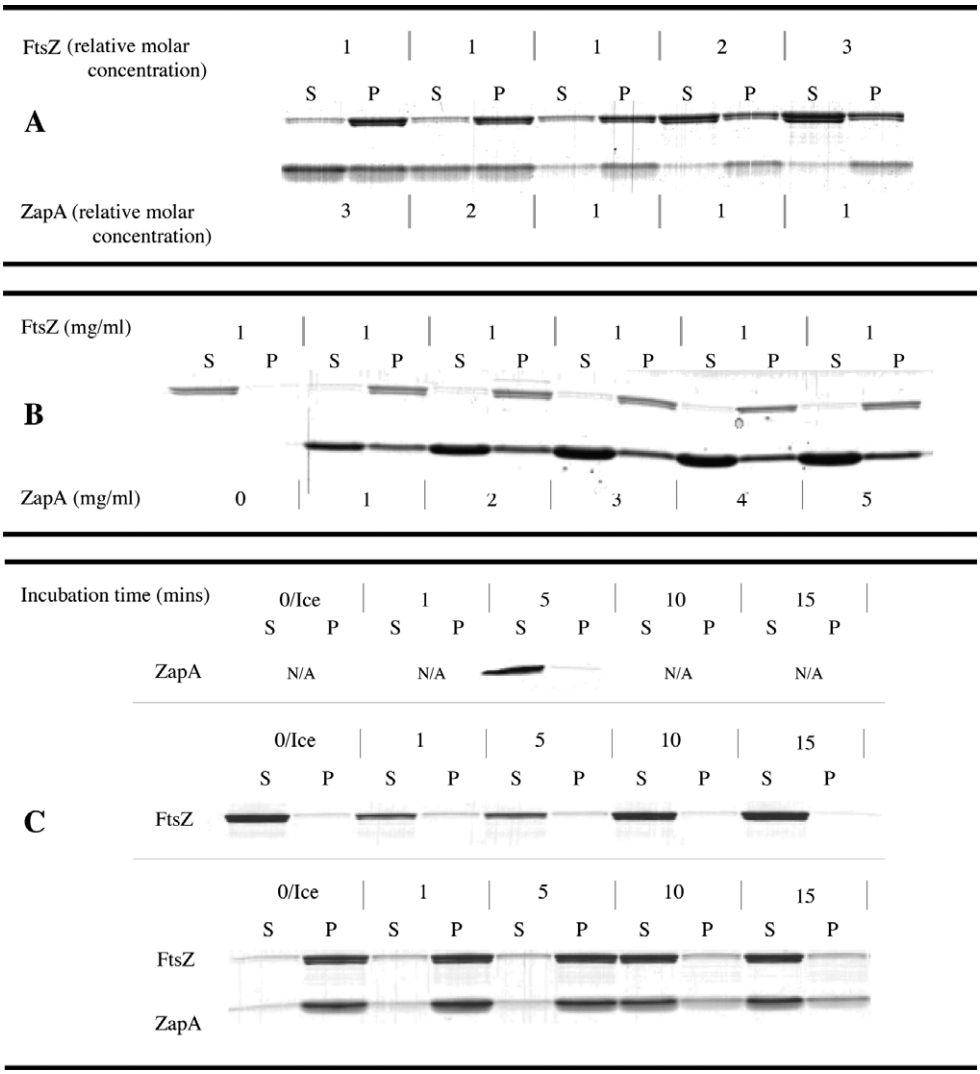

Figure 4. FtsZ and ZapA pelleting assays. P = pellet, S = supernatant. A, Titration of FtsZ against ZapA and *vice versa* from a threefold excess. Only at equal molarity (5 μM protein concentration) does all ZapA and FtsZ localise predominantly in the pellet signifying a 1 : 1 inter-molecule binding ratio. B, Confirmation of stoichiometric relationship observed in A: titration of ZapA against FtsZ (mg/ml). ZapA in greater than 1 : 1 ratio with FtsZ collects quantitatively in the supernatant. At 1 : 1 ratio the ZapA supernatant band has approximately twice the volume of the pellet band reflecting the different molecular masses of His_6-ZapA (12.6 kDa) and FtsZ (41 kDa). C, Effect of ZapA on FtsZ polymer stability. ZapA localises in the supernatant when independent of FtsZ (T = five minutes only; NA = not attempted) (top). Incubation of FtsZ alone; polymers are of insufficient size and stability to pellet and so localise in the supernatant alone (middle). FtsZ filaments are stabilised for between five and ten minutes in the presence of ZapA and together they localise in the pellet. After ten minutes the FtsZ polymers have dissociated, and both proteins accumulate in the supernatant (bottom). Protein concentration is 15 μM for FtsZ and ZapA.

(41 kDa) is approximately 3.25 times greater than a His_6-ZapA molecule (12.6 kDa)) that ZapA be present in a supernatant to pellet ratio of 2.25 : 1. Indeed, quantification analysis of the ZapA bands shows almost exactly this ratio; at 1 mg/ml the supernatant band has a volume that is 2.0 times the pellet band. Therefore, it is clear that at equal molarities, FtsZ and ZapA likely associate stoichiometrically with a ratio close to 1 : 1, and that the ZapA dimer or tetramer has the capability of binding up to two or four FtsZ molecules, respectively. When levels of ZapA are increased up to a five times excess, unbound ZapA collects proportionately in the supernatant. The quantity of pelleted ZapA is seen to slightly increase and this is likely due to a FtsZ super-saturation effect. Finally, to probe the affinity of ZapA for FtsZ and to determine the temporal longevity of its stabilising effect on filaments, the two proteins were incubated over a time course of 15 minutes in the presence of GTP before centrifugation (Figure 4C). When FtsZ alone is incubated, probably due to strict GTP-dependent polymerisation[26,46] and a high GTP turnover of *P. aeruginosa* FtsZ, the protein fails to localise in the pellet at all time-points. In stark contrast, FtsZ in combination with ZapA is filamentous and stable during the first five minutes of incubation and thus localises in the pellet. After

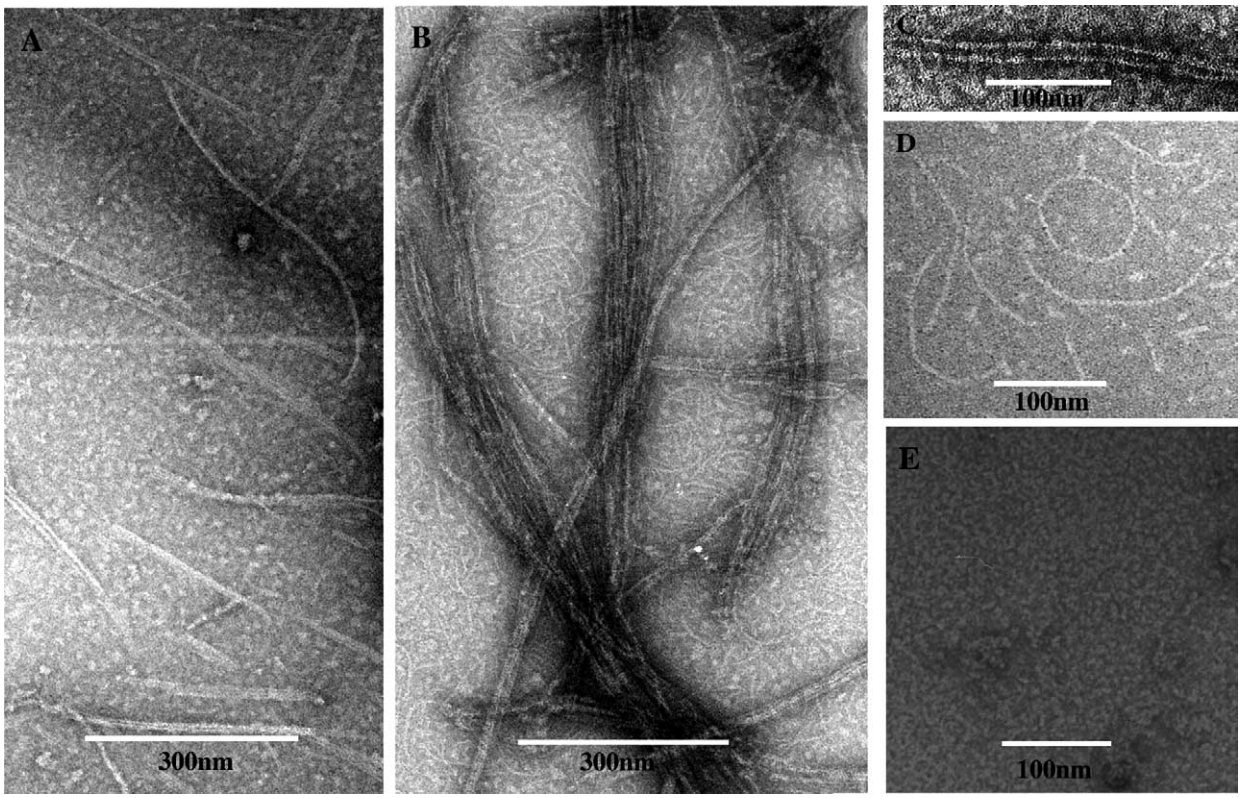

Figure 5. Negative stain electron microscopy of FtsZ alone and in combination with ZapA: A, 0.6 mg/ml FtsZ plus 2 mM GTP; B, 0.6 mg/ml FtsZ, 2 mM GTP plus 0.2 mg/ml ZapA; note increase in bundling. C, Similar conditions to B; high magnification of a putative tube-like filament. D, Similar to B but focusing on the smaller protofilaments found in abundance in the background. E, FtsZ control; as A, but with no GTP.

this time, there is an absence of pelleting and the two proteins localise solely to the supernatant.

Electron microscopy

Previous study of ZapA–FtsZ interaction by negative stain electron microscopy has focused on the *B. subtilis* system in which ZapA was first discovered.[45] *P. aeruginosa* FtsZ has extremely high GTPase kinetics and consequently high rates of polymer formation and dissociation. Given strong correlation between micrographs in this study and in the original paper, ZapA seems to have a homologous effect on FtsZ despite the change in organism. Incubation of FtsZ and GTP alone at 37 °C yielded single short protofilaments which usually joined laterally to form paired protofilaments and small bundles. Small oligomers are present in the background (Figure 5A). In contrast, the presence of ZapA in stoichiometric balance with FtsZ provoked dramatic formation of an elongated heavily bundled fibrous network over the grid (Figure 5B) similar to that observed previously.[45] Such bundles predominantly consisted of filaments that could be akin to the helical tubes obtained in the presence of DEAE-dextran and nucleotide (Figure 5C).[23] In the background to the bundles, or as a consequence of reduced incubation time, there are many single curled protofilaments (Figure 5D). Diffraction analysis was impeded by a deficit of order and resolution within the tube-like structures as a consequence of heavy bundling. Diffraction analysis therefore failed to give insight into the positioning and orientation of ZapA in relation to the FtsZ protofilaments.

Discussion

The crystal structure of ZapA shows two dimers that associate to yield an anti-parallel tetramer. Formation of the tetramer could be irrelevant *in vivo* given the dimer is the dominant species at lower and possibly more physiologically relevant protein concentrations. Irrespective of oligomerisation state, however, it may be predicted that 1 mol of ZapA monomer might bind 0.5 or 1 mol of FtsZ. In accordance, the pelleting assays (Figure 4A and B) indicate that an equal stoichiometry between monomeric FtsZ and ZapA is reasonable. Such observation concurs with a previously reported light-scattering assay.[45] One ZapA dimer (or tetramer) should be able to bind up to two (or four) FtsZ molecules *in vivo*, with each subunit or their interface contributing one binding site. Thus, in this study, we show in *P. aeruginosa* that ZapA promotes FtsZ polymerisation, filament formation and stabilisation by forming a dimer that

engages FtsZ molecules with an approximate 1 : 1 stoichiometry. In addition, the propensity of the ZapA dimer to form a tetramer suggests a two-stage FtsZ cross-linking mechanism. In this model, as Z-ring assembly initiates, ZapA dimer binds and cross-links FtsZ polymer that is integrated into the growing ring. Integration within the Z-ring would result in a significant increase in local concentration of ZapA dimer. It has been estimated that ZapA concentration is 5% that of FtsZ, so that ZapA may be found bound to one in every 20 FtsZ monomers.[45] If local concentration becomes sufficiently high, ultracentrifugation data (Figure 1A–E) show that ZapA dimer–tetramer equilibrium shifts considerably towards that of the higher-order oligomeric state. Inter-dimer association would then provide a secondary mode of FtsZ cross-linking that would greatly enhance the ability of ZapA to stabilise and compact the Z-ring. Such a mechanism would complement the apparent cooperative self assembly of FtsZ *in vitro*.[47]

Examination of the surface electrostatic potential of the ZapA dimer shows it to be dominated by an area of negative charge localising to the N terminus of helix H1 and its contact with helix H2 (Figure 6A). The C-terminal α-helices also have a predominantly acidic nature. Formation of the tetramer shifts the surface charge so that each dimer is dominated by a basic region located at the tip of the globular terminus along a central groove. Two different conformations seem to exist on each side of the dimer, as this central groove is slightly occluded on the reverse side. It is therefore postulated that the globular domain of ZapA oligomers mediates FtsZ interaction. Eukaryotic microtubule-associated proteins (MAPs) such as Tau, MAP2 and MAP4 play a similar role to ZapA in that they promote tubulin polymerisation, stabilise microtubules (MTs) and have propensity to induce bundle formation when over-expressed.[48] However, although Tau,[49] MAP2[50] and the juvenile form MAP2c[51] are known to form dimers of an anti-parallel nature and to contain multiple binding sites as in the ZapA tetramer, there is no sequence homology between ZapA and MAPs and their *modus operandi* is likely quite different. It is of interest to note, however, that MAPs utilise basic microtubule-binding domains that bind to the acidic C termini of αβ-tubulin.[48] FtsZ has a similarly negative C terminus (although highly diverged from tubulin and whose terminal 67 residues are non-essential for polymerisation in *E. coli*)[4] localising on helix H10.[7] If ZapA dimer does self-associate into tetramer, such acidic areas upon the FtsZ surface could stabilise the more basic character of the ZapA tetramer.

Further evidence that the globular terminus of ZapA mediates its interaction with FtsZ comes from a grading of inter-species residue conservation from 25 organisms containing ZapA (Figure 6B). This diagram reveals an area comparatively free from evolutionary restraint located and confined to the C-terminal surfaces of the H2 helices around the tetramerisation domain. Importantly, such observation tends to hold for the molecules directed towards the exterior surface (dark blue residues), which strongly suggests that FtsZ binding is not dependent upon this surface. Residues coating the internal face of the H2 helices show a stronger degree of conservation than the exterior, which would be expected if this area mediates tetramerisation *in vivo*. The globular terminus of the molecule exhibits in general a much higher degree of residue conservation and emerges as the natural candidate for mediating FtsZ binding.

Of considerable interest, especially given the potential ramifications for the nature of the Z-ring itself, is the symmetry of the ZapA oligomers. Whilst the dimer has a single 2-fold, the bipolar tetramer has three (222 symmetry). Consider tubulin and FtsZ, both of which have been visualised at atomic resolution. The αβ-tubulin crystal structure was solved from Zn-stimulated anti-parallel

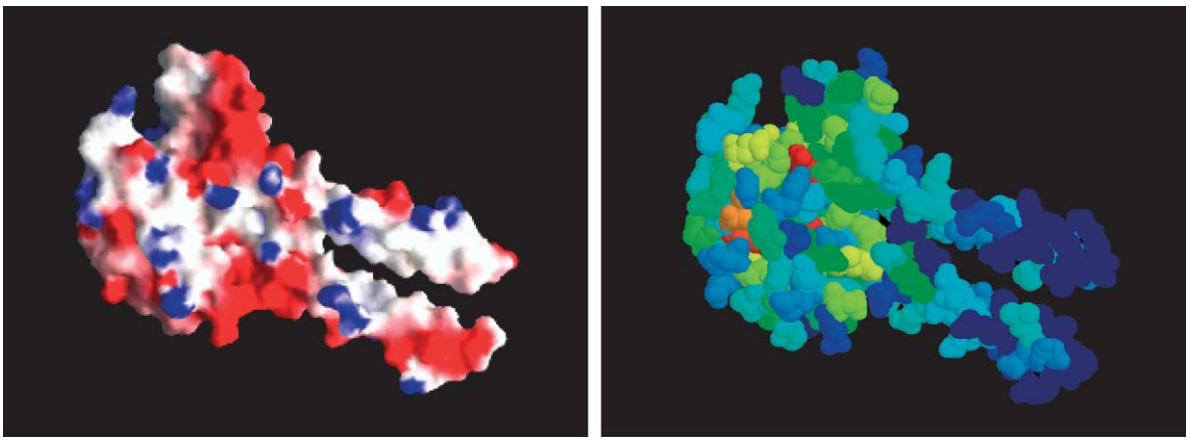

Figure 6. A, Surface map displaying the electrostatic potential of the ZapA dimer. Coloured from −6.0 kT/e, red to 6.0 kT/e, blue. Orientation is similar to subunits AB in Figure 2B. B, A grading of inter-species residue conservation from 25 ZapA sequences; a spectrum from red, highly conserved through to dark blue, least conserved. Orientation is similar to subunits AB in Figure 2B.

protofilaments which gave direct information about longitudinal inter-subunit contact.[52] In contrast, the FtsZ crystal structure required it to be superimposed into reconstructed Ca^{2+}-induced sheets, also anti-parallel in nature, before detail of longitudinal interaction could be educed.[22] During polymerisation, both αβ-tubulin and FtsZ depend on the T7 loop from a neighbouring molecule to contact and facilitate activation of the polymerisation-dependent GTPase. Such specific interaction forces strict head–tail polarity on these dynamic systems. EM studies show that FtsZ in combination with ZapA yields not only heavily bundled filaments but also single smaller protofilaments (Figure 5B and D). Such single protofilaments appear to be relatively unstable when ZapA is absent and so tend to associate as pairs or small bundles (Figure 5A). Therefore, an attractive working model for the ZapA dimer would have it binding along single FtsZ protofilaments either corrupting the depolymerising effect of the GTPase itself[26] or simply providing mechanical stability by acting as a molecular splint. However, this is improbable given the symmetry of the dimer and strict polarity of FtsZ assembly. Instead, ZapA dimer likely functions as a molecular bridge acting between two protofilaments. Binding to a single protofilament with just one of its binding sites would be sufficient to provide local stability. FtsZ protofilaments have no 2-fold symmetry and so their polarity or direction should be dictated and restrained upon interaction with a ZapA dimer. Protofilaments may therefore be arranged anti-parallel with each other with the H2 helices of ZapA perpendicular to the filaments (Figure 7B1); or they may run in the same direction as each other (but must be related by a 180° rotation in this plane) and have the H2 helices of ZapA aligned in parallel (Figure 7A1). If *in vivo*, FtsZ cross-linking is mediated by both ZapA dimer and tetramer, any two pairs of dimer-associated protofilaments must be oriented so that they also satisfy the symmetry requirements of the tetramer (Figure 7A2 and B2). With such reconciliation between ZapA symmetry and polarity of associated FtsZ polymer, what implications are there for Z-ring architecture *in vivo*?

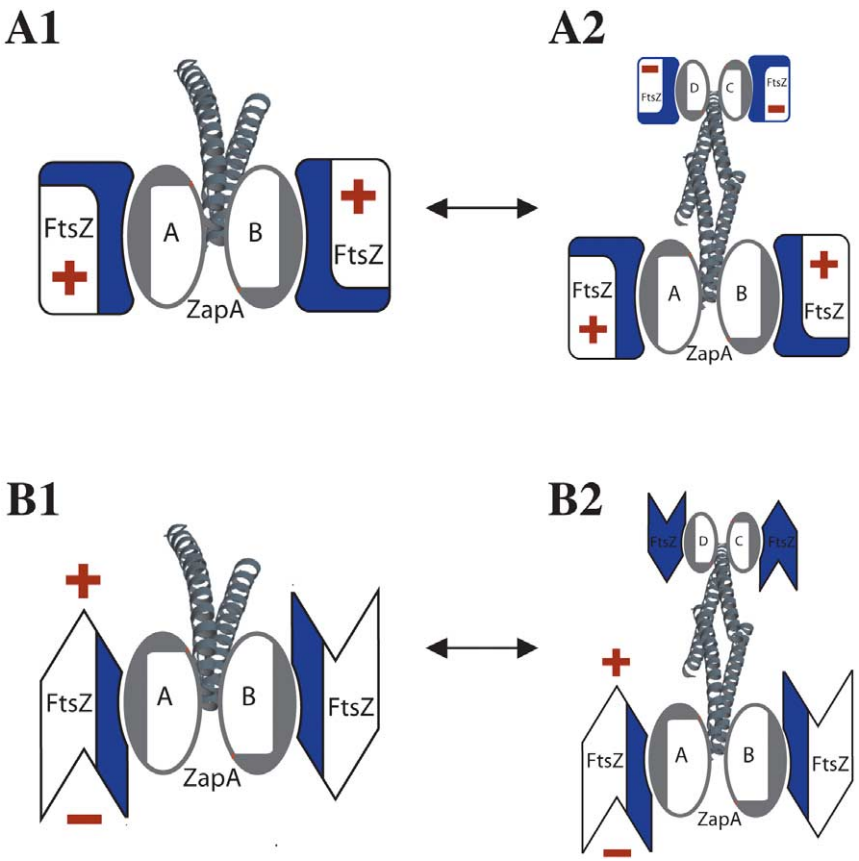

Figure 7. A non-exhaustive analysis showing how ZapA dimer or tetramer may dictate the orientation of FtsZ protofilaments. ZapA is oriented with its long axis along the *Z*-axis into the page (perfect symmetry is assumed). " + " and " − " correspond to the polarity of FtsZ molecules within a protofilament. A1, ZapA dimer cross-links a pair of parallel protofilaments that are related by a 180° rotation around the *Z*-axis. ZapA H2 helices run in parallel with the filaments. A2, ZapA tetramer formed from A1 inter-dimer association. Tetramerisation yields two pairs of FtsZ filaments that run anti-parallel with each other. Flexibility in the globular heads of ZapA would allow opposing filaments to "slide" over each other. B1, ZapA dimer cross-links a pair of anti-parallel protofilaments. ZapA H2 helices run perpendicular to the length of the filaments. B2, ZapA tetramer formed from B1 inter-dimer association. The tetramer cross-links two opposing pairs of anti-parallel FtsZ filaments.

Given ZapA has been shown to localise over the whole Z-ring,[45] the symmetry of this molecule likely demands a Z-ring with a high content of filaments arranged anti-parallel with each other (for example, Figure 7A2, B1 and B2). Interestingly, anti-parallel FtsZ protofilaments have been demonstrated *in vitro*. Using a GFP-FtsZ chimera in the presence of Ca^{2+}, FtsZ protofilaments were shown to originate from nucleation centres that grow into large web-like networks that bear a striking resemblance to eukaryotic MT asters.[25] Such protofilaments, nucleated over 10 μm away from each other, connect *via* an attraction that is likely to be of a lateral rather than a head–head or head–tail nature. What is critical here is that merged bundles would be a combination of protofilaments with opposite polarity associating laterally (reminiscent of non-kinetochore MTs overlapping in mitosis). Given there are between 3200[53] and 15,000[54] FtsZ monomers in an *E. coli* cell, there is thought to be sufficient polymer to encircle the cell multiple times. The Z-ring can therefore, in theory, comprise a single ring formed from multiple anti-parallel protofilaments associating laterally. Such a design would be compatible with ZapA dimer and tetramer.

This kind of anti-parallel ring architecture *in vivo* could be achieved *via* multiple bi-directional nucleation sites of the nature described by Yu and Margolin[25] distributed around the mid cell, or by a single bi-directional nucleation site as has been observed.[55] If there is just a single nucleation site, an initial seed of a few bi-directional filaments must encircle the cell multiple times if ZapA is to associate over the entire ring. Such a ring would manifest as a circumferential bi-directional helix. In this respect, it has been reported that when *B. subtilis* switch their medial Z-ring to a polar location during asymmetric cell division, the medial Z-ring is converted into a helical-like filament that grows bi-directionally along the long axis of the cell.[5] Such observation combined with the design of ZapA naturally infers the medial Z-ring itself is assembled as a condensed and tightly cross-linked bi-directional helix. During asymmetric division, inhibition of ZapA and other cross-linking molecules such as ZipA could relax the helix, thereby increasing its pitch and promoting its relocation to the poles. In addition, over-expression of FtsZ in combination with FtsZ-GFP has been shown to induce a switch from a localised functional Z-ring to a helical structure that extends the length of the cell in *E. coli*.[4] Such over-expression may reflect the inability of the cell to contain the medial Z-ring in a condensed form, possibly due to a deficiency in the relative concentration of proteins involved in cross-linking.

The design of ZapA can also be understood and its symmetry functionally fulfilled, if the filaments that constitute the Z-ring have a helical morphology. In *Methanococcus jannaschii* FtsZ in the presence of GMPCPP, helical tubes seemingly comprising three independent groups of four anti-parallel thick filaments (paired parallel protofilaments) have been reported.[24] ZapA (dimer and tetramer) could stabilise FtsZ by either decorating the internal face of such a helix in a similar manner to the MAP Tau[56] and promote inter-filament bundling indirectly, or by simply binding to the exterior and mediating cross-linking directly. Other tubular polymers of FtsZ *in vitro* are also known and their substructure has been described.[23,24,57] However, the idea of a helical Z-ring may be less likely given such architecture is predominantly favoured when FtsZ is GDP associated.[21,23] In accordance, although ZapA has been shown capable of driving FtsZ polymerisation in the presence of GDP,[45] the pelleting assay time-course (Figure 4C) indicates FtsZ filaments are unstable over time, presumably as GTP is hydrolysed and is replaced by GDP.

ZapA is not the only known anti-parallel molecule involved in the division system that is capable of direct binding to FtsZ. The Z-ring inhibitor SulA forms an anti-parallel dimer[35] that caps FtsZ filaments by binding to the T7 loop and physically blocking polymer elongation. Critically, the SulA–FtsZ binding site is directly opposite the SulA dimer interface which results in bound FtsZ monomers or filaments with exactly opposing polarity. Thus, it has been proposed that SulA could have the ability to crosslink FtsZ protofilaments but only by "imposing" bipolar symmetry on the filaments. Imposition of filament symmetry is unnecessary, however, and would be complementary instead, if the Z-ring originates with anti-parallel orientation by growing bi-directionally from either single or multiple nucleation points as discussed above. With a high turnover of FtsZ molecules, between those filamentous in the Z-ring and those unbound in the cytosol,[27] the requirement for SulA to have an anti-parallel design is more easily understood. The dimer would be ideally orientated to cap opposing filaments within the Z-ring, to isolate and contain large sections and to rapidly provoke its collapse during the SOS response.

This study shows that ZapA employs at least a dimer in its modulation of FtsZ and Z-ring dynamics. Through an ability to bind FtsZ with 1 : 1 stoichiometry, the dimer stabilises and cross-links FtsZ polymers and likely functions as a molecular bridge acting between FtsZ protofilaments rather than binding along their length. A two-stage FtsZ cross-linking mechanism that is concentration-dependent may involve ZapA inter-dimer association to form a bipolar tetramer. In addition, the symmetry and the association of ZapA over the entire Z-ring may dictate that ZapA will only stabilise and bundle FtsZ filaments orientated anti-parallel with each other. It is possible therefore that the Z-ring is either a circumferential tightly cross-linked bi-directional helix; or else is formed from tubule-like filaments with helical morphology. Elucidating the site of ZapA–FtsZ interaction and the relative orientations of the FtsZ polymer is not easy due to the dynamic and transient nature

of this system. However, pursuit of such understanding is important if the Z-ring ultra-structure is to be understood.

Materials and Methods

Protein expression, purification and crystallisation

Pseudomonas aeruginosa PA01-LAC *zapA* (accession number ATCC47085D) was amplified using the polymerase chain reaction (PCR) from genomic DNA with the primers 5′-TGACTACCATATGAGCCAGTCGAATA CCCTCACCGTGC-3′ and 5′-AGTCTACGGATCCGGCT TCGCCGGCATCGGCCGGATTCG-3′. NdeI and BamHI treated fragments were cloned into pHis-17 vector yielding a 112 amino acid residue protein with a C-terminal extension of eight residues (GSHHHHHH). Transformed C41(DE3)[58] cells were grown at 37 °C in 2 × TY medium containing 100 μg/ml of ampicillin and induced with 1 mM isopropyl-β-D-thiogalactosidase (IPTG) at $A_{600} = 0.5$. After four hours, cells were centrifuged and frozen in liquid nitrogen. Cells thawed in 50 mM Tris–HCl (pH 8.0) were treated with DNase I, lysozyme and sonicated. After centrifugation, the supernatant was passed over a Ni^{2+}-NTA column (Qiagen). The column was washed with 50 mM Tris–HCl (pH 6.0), 300 mM NaCl and 20 mM imidazole. ZapA was eluted with 100–300 mM imidazole in the same buffer. Peak fractions were concentrated and loaded onto a Sephacryl S200 gel-filtration column (Amersham) equilibrated in 20 mM Tris–HCl (pH 7.5), 1 mM EDTA and 1 mM NaN_3. Concentrated protein at 50 mg/ml was stored at −80 °C.

For selenomethionine-substituted ZapA, M9 minimal medium supplemented with 0.4% (w/v) glucose, 2 mM $MgSO_4$ and 100 μg/ml of ampicillin was inoculated and grown to $A_{600} = 0.3$. DL-Selenomethionine (Sigma: 100 mg/l), 100 mg/l of lysine, threonine and phenylalanine, and 50 mg/l of leucine, isoleucine and valine were then added as solids. Fifteen minutes later, cells were induced with 1 mM IPTG and grown overnight. Protein purification was as for the unsubstituted protein except buffers were supplemented either with 5 mM dithiothreitol (DTT) or, if in contact with Ni^{2+}-NTA, with 5 mM β-mercaptoethanol. The purified protein was confirmed by N-terminal sequencing and electrospray mass spectrometry (ZapA minus N-terminal methionine: observed 12,492 Da, calculated 12,490 Da). Crystals were grown using the sitting-drop, vapour-diffusion technique in 0.1 M imidazole (pH 7.0) and 30% (v/v) MPD (2-methyl-2,4-pentanediol). One microliter of 50 mg/ml protein was mixed with an equal volume of crystallisation solution and left to equilibrate for 36 hours. Crystals grew in space group $P4_12_12$ with cell dimensions $a = b = 105.2$ Å, $c = 36.0$ Å and two molecules in the asymmetric unit.

Pseudomonas aeruginosa FtsZ was cloned into pHis-17 with primers that excluded the vector-encoded polyhistidine tag to yield full-length untagged protein. Expression was as for ZapA except 1% glucose was added to the growth medium. See Rivas *et al.* for the method of protein purification.[59] Protein was gel-filtered using a Sephacryl S300 column (Amersham) equilibrated in 20 mM Tris–HCl (pH 7.4), 1 mM EDTA and 1 mM NaN_3. Concentrated protein at 10 mg/ml was stored at −80 °C.

Structure determination and refinement

All data were collected on beam-line 14-2 at the Daresbury SRS and were indexed and integrated with the MOSFLM package[60] and further processed with the CCP4 suite of programs.[61] Identification of two out of a possible three selenium atoms was determined and phased by SOLVE.[62] RESOLVE was used for solvent flattening with a solvent content of 51% (v/v). The model was built using MAIN[63] and refined using CNS with Engh & Huber stereochemical parameters.[64]

Chromatography, mass spectrometry and sedimentation velocity analytical ultracentrifugation

Chromatography: 10 μl of five protein standards (see Figure 1G) at 2 mg/ml were injected onto a Biosep SEC S3000 column equilibrated in 20 mM Tris (pH 7.5), 200 mM NaCl and 5 mM $MgCl_2$ and eluted separately. Following calibration, 10 μl of ZapA protein at 10 mg/ml was injected and eluted as a single species from the column. Mass spectrometry: ZapA was sprayed into a TOF2 tandem mass spectrometer modified for high mass operation[65] at 25 μM using gold-coated borosilicate nanoflow capillaries in 50 mM ammonium acetate (pH 7.5). Sedimentation velocity analytical ultracentrifugation: experiments were performed using a Beckman Optima XL-A analytical ultracentrifuge equipped with absorbance and interference optics. ZapA (410 μl) in 20 mM Tris (pH 7.5), 1 mM EDTA, 1 mM NaN_3 and 200 mM NaCl was placed in the sample compartment of an Epon double-sector centerpiece and an equal volume of the same solution without protein was placed in the reference compartment. The samples were centrifuged at 293 K and 45,000 rpm using an An60-Ti rotor. Scans were acquired at intervals of three minutes. The calculated partial specific volume derived from the amino acid composition of ZapA (0.7177 g^{-1}/cm^3), buffer density (1.01 g/cm^3) and viscosity (0.01003 P) were obtained using SEDNTERP.[66] $c(S)$ and $c(M)$ distributions were calculated using the program SEDFIT.[67]

Pelleting assays

Purified FtsZ and ZapA were mixed in 30 μl reactions with buffer A (100 mM Pipes (pH 6.8), 2 mM $MgCl_2$), 2 mM GTP and incubated for five minutes at 37 °C (unless otherwise stated). For specific protein concentrations please refer to the legend in Figure 4. The reactions were centrifuged at 100 K in a Beckman TLA100 rotor for 15 minutes at 4 °C. Without centrifugation at low temperature, the high reaction kinetics of *P. aeruginosa* induces filament depolymerisation before analysis is possible. The 30 μl supernatant was removed and mixed with an equal volume of SDS-containing loading buffer. The pellet was washed in 30 μl of buffer A, and then solubilised in a 60 μl 1 : 1 mixture of the above loading buffer and buffer A. Supernatant and pellets were analysed using SDS PAGE (18% (w/v) polyacrylamide) (Biorad). The software ImageQuant was used to quantify the band volumes.

Electron microscopy

FtsZ (0.6 mg/ml) mixed with 0.2 mg/ml of ZapA (when applicable) in 30 μl reactions with buffer B (100 mM Mes (pH 6.2), 2 mM $MgCl_2$, 2 mM GTP was

incubated for five minutes at 37 °C. A portion (10 μl) of the reaction was placed onto a carbon-coated copper electron microscope grid. Excess liquid was blotted off. Having washed the grids with a drop of water, they were stained with three drops of 1.5% (w/v) uranyl acetate. Pictures were taken with a Philips 208 electron microscope on film plates. Magnification was from 20,000× to 50,000×. Images were digitised on a Zeiss SCAI CCD scanner.

Acknowledgements

We thank Linda A. Amos for helpful discussions; Sew Peak-chew for N-terminal sequencing (MRC Laboratory of Molecular Biology, Cambridge, UK); and Frank Sobott and Carol V. Robinson for mass spectrometry (Department of Chemistry, Cambridge University, UK).

References

1. Bi, E. F. & Lutkenhaus, J. (1991). FtsZ ring structure associated with division in *Escherichia coli*. *Nature*, **354**, 161–164.
2. Levin, P. A. & Losick, R. (1996). Transcription factor Spo0A switches the localization of the cell division protein FtsZ from a medial to a bipolar pattern in *Bacillus subtilis*. *Genes Dev.* **10**, 478–488.
3. Addinall, S. G., Bi, E. & Lutkenhaus, J. (1996). FtsZ ring formation in fts mutants. *J. Bacteriol.* **178**, 3877–3884.
4. Ma, X., Ehrhardt, D. W. & Margolin, W. (1996). Colocalization of cell division proteins FtsZ and FtsA to cytoskeletal structures in living *Escherichia coli* cells by using green fluorescent protein. *Proc. Natl Acad. Sci. USA*, **93**, 12998–13003.
5. Ben-Yehuda, S. & Losick, R. (2002). Asymmetric cell division in *B. subtilis* involves a spiral-like intermediate of the cytokinetic protein FtsZ. *Cell*, **109**, 257–266.
6. Löwe, J. & Amos, L. A. (1998). Crystal structure of the bacterial cell-division protein FtsZ. *Nature*, **391**, 203–206.
7. Nogales, E., Downing, K. H., Amos, L. A. & Löwe, J. (1998). Tubulin and FtsZ form a distinct family of GTPases. *Nature Struct. Biol.* **5**, 451–458.
8. Erickson, H. P. (1998). Atomic structures of tubulin and FtsZ. *Trends Cell. Biol.* **8**, 133–137.
9. van den Ent, F., Amos, L. A. & Löwe, J. (2001). Prokaryotic origin of the actin cytoskeleton. *Nature*, **413**, 39–44.
10. Jones, L. J., Carballido-Lopez, R. & Errington, J. (2001). Control of cell shape in bacteria: helical, actin-like filaments in *Bacillus subtilis*. *Cell*, **104**, 913–922.
11. Ausmees, N., Kuhn, J. R. & Jacobs-Wagner, C. (2003). The bacterial cytoskeleton: an intermediate filament-like function in cell shape. *Cell*, **115**, 705–713.
12. Margolin, W. (2000). Themes and variations in prokaryotic cell division. *FEMS Microbiol. Rev.* **24**, 531–548.
13. Rothfield, L., Justice, S. & Garcia-Lara, J. (1999). Bacterial cell division. *Annu. Rev. Genet.* **33**, 423–448.
14. Osteryoung, K. W., Stokes, K. D., Rutherford, S. M., Percival, A. L. & Lee, W. Y. (1998). Chloroplast division in higher plants requires members of two functionally divergent gene families with homology to bacterial ftsZ. *Plant Cell*, **10**, 1991–2004.
15. Beech, P. L., Nheu, T., Schultz, T., Herbert, S., Lithgow, T., Gilson, P. R. & McFadden, G. I. (2000). Mitochondrial FtsZ in a chromophyte alga. *Science*, **287**, 1276–1279.
16. Nishida, K., Takahara, M., Miyagishima, S. Y., Kuroiwa, H., Matsuzaki, M. & Kuroiwa, T. (2003). Dynamic recruitment of dynamin for final mitochondrial severance in a primitive red alga. *Proc. Natl Acad. Sci. USA*, **100**, 2146–2151.
17. Addinall, S. G. & Holland, B. (2002). The tubulin ancestor, FtsZ, draughtsman, designer and driving force for bacterial cytokinesis. *J. Mol. Biol.* **318**, 219–236.
18. Romberg, L. & Levin, P. A. (2003). Assembly dynamics of the bacterial cell division protein FTSZ: poised at the edge of stability. *Annu. Rev. Microbiol.* **57**, 125–154.
19. Buddelmeijer, N. & Beckwith, J. (2002). Assembly of cell division proteins at the *E. coli* cell center. *Curr. Opin. Microbiol.* **5**, 553–557.
20. Errington, J., Daniel, R. A. & Scheffers, D. J. (2003). Cytokinesis in bacteria. *Microbiol. Mol. Biol. Rev.* **67**, 52–65. table of contents..
21. Erickson, H. P., Taylor, D. W., Taylor, K. A. & Bramhill, D. (1996). Bacterial cell division protein FtsZ assembles into protofilament sheets and minirings, structural homologs of tubulin polymers. *Proc. Natl Acad. Sci. USA*, **93**, 519–523.
22. Löwe, J. & Amos, L. A. (1999). Tubulin-like protofilaments in Ca^{2+}-induced FtsZ sheets. *EMBO J.* **18**, 2364–2371.
23. Lu, C., Reedy, M. & Erickson, H. P. (2000). Straight and curved conformations of FtsZ are regulated by GTP hydrolysis. *J. Bacteriol.* **182**, 164–170.
24. Löwe, J. & Amos, L. A. (2000). Helical tubes of FtsZ from *Methanococcus jannaschii*. *Biol. Chem.* **381**, 993–999.
25. Yu, X. C. & Margolin, W. (1997). Ca^{2+}-mediated GTP-dependent dynamic assembly of bacterial cell division protein FtsZ into asters and polymer networks *in vitro*. *EMBO J.* **16**, 5455–5463.
26. Mukherjee, A. & Lutkenhaus, J. (1998). Dynamic assembly of FtsZ regulated by GTP hydrolysis. *EMBO J.* **17**, 462–469.
27. Stricker, J., Maddox, P., Salmon, E. D. & Erickson, H. P. (2002). Rapid assembly dynamics of the *Escherichia coli* FtsZ-ring demonstrated by fluorescence recovery after photobleaching. *Proc. Natl Acad. Sci. USA*, **99**, 3171–3175.
28. Scheffers, D. J., de Wit, J. G., den Blaauwen, T. & Driessen, A. J. (2002). GTP hydrolysis of cell division protein FtsZ: evidence that the active site is formed by the association of monomers. *Biochemistry*, **41**, 521–529.
29. Lu, C., Stricker, J. & Erickson, H. P. (2001). Site-specific mutations of FtsZ–effects on GTPase and *in vitro* assembly. *BMC Microbiol.* **1**, 7.
30. Raskin, D. M. & de Boer, P. A. (1997). The MinE ring: an FtsZ-independent cell structure required for selection of the correct division site in *E. coli*. *Cell*, **91**, 685–694.
31. Raskin, D. M. & de Boer, P. A. (1999). Rapid pole-to-pole oscillation of a protein required for directing

division to the middle of *Escherichia coli*. *Proc. Natl Acad. Sci. USA*, **96**, 4971–4976.
32. Marston, A. L. & Errington, J. (1999). Selection of the midcell division site in *Bacillus subtilis* through MinD-dependent polar localization and activation of MinC. *Mol. Microbiol.* **33**, 84–96.
33. Marston, A. L., Thomaides, H. B., Edwards, D. H., Sharpe, M. E. & Errington, J. (1998). Polar localization of the MinD protein of *Bacillus subtilis* and its role in selection of the mid-cell division site. *Genes Dev.* **12**, 3419–3430.
34. Levin, P. A., Kurtser, I. G. & Grossman, A. D. (1999). Identification and characterization of a negative regulator of FtsZ ring formation in *Bacillus subtilis*. *Proc. Natl Acad. Sci. USA*, **96**, 9642–9647.
35. Cordell, S. C., Robinson, E. J. & Löwe, J. (2003). Crystal structure of the SOS cell division inhibitor SulA and in complex with FtsZ. *Proc. Natl Acad. Sci. USA*, **100**, 7889–7894.
36. Bi, E. & Lutkenhaus, J. (1993). Cell division inhibitors SulA and MinCD prevent formation of the FtsZ ring. *J. Bacteriol.* **175**, 1118–1125.
37. Jones, C. & Holland, I. B. (1985). Role of the SulB (FtsZ) protein in division inhibition during the SOS response in *Escherichia coli*: FtsZ stabilizes the inhibitor SulA in maxicells. *Proc. Natl Acad. Sci. USA*, **82**, 6045–6049.
38. Wang, X., Huang, J., Mukherjee, A., Cao, C. & Lutkenhaus, J. (1997). Analysis of the interaction of FtsZ with itself, GTP, and FtsA. *J. Bacteriol.* **179**, 5551–5559.
39. Pichoff, S. & Lutkenhaus, J. (2002). Unique and overlapping roles for ZipA and FtsA in septal ring assembly in *Escherichia coli*. *EMBO J.* **21**, 685–693.
40. Feucht, A., Lucet, I., Yudkin, M. D. & Errington, J. (2001). Cytological and biochemical characterization of the FtsA cell division protein of *Bacillus subtilis*. *Mol. Microbiol.* **40**, 115–125.
41. Hale, C. A. & de Boer, P. A. (2002). ZipA is required for recruitment of FtsK, FtsQ, FtsL, and FtsN to the septal ring in *Escherichia coli*. *J. Bacteriol.* **184**, 2552–2556.
42. Hale, C. A. & de Boer, P. A. (1997). Direct binding of FtsZ to ZipA, an essential component of the septal ring structure that mediates cell division in *E. coli*. *Cell*, **88**, 175–185.
43. Hale, C. A., Rhee, A. C. & de Boer, P. A. (2000). ZipA-induced bundling of FtsZ polymers mediated by an interaction between C-terminal domains. *J. Bacteriol.* **182**, 5153–5166.
44. RayChaudhuri, D. (1999). ZipA is a MAP-Tau homolog and is essential for structural integrity of the cytokinetic FtsZ ring during bacterial cell division. *EMBO J.* **18**, 2372–2383.
45. Gueiros-Filho, F. J. & Losick, R. (2002). A widely conserved bacterial cell division protein that promotes assembly of the tubulin-like protein FtsZ. *Genes. Dev.* **16**, 2544–2556.
46. Mukherjee, A. & Lutkenhaus, J. (1994). Guanine nucleotide-dependent assembly of FtsZ into filaments. *J. Bacteriol.* **176**, 2754–2758.
47. Caplan, M. R. & Erickson, H. P. (2003). Apparent cooperative assembly of the bacterial cell division protein FtsZ demonstrated by isothermal titration calorimetry. *J. Biol. Chem.* **278**, 13784–13788.
48. Chapin, S. J. & Bulinski, J. C. (1992). Microtubule stabilization by assembly-promoting microtubule-associated proteins: a repeat performance. *Cell Motil. Cytoskeleton*, **23**, 236–243.
49. Wille, H., Drewes, G., Biernat, J., Mandelkow, E. M. & Mandelkow, E. (1992). Alzheimer-like paired helical filaments and antiparallel dimers formed from microtubule-associated protein tau *in vitro*. *J. Cell Biol.* **118**, 573–584.
50. Wille, H., Mandelkow, E. M., Dingus, J., Vallee, R. B., Binder, L. I. & Mandelkow, E. (1992). Domain structure and antiparallel dimers of microtubule-associated protein 2 (MAP2). *J. Struct. Biol.* **108**, 49–61.
51. Wille, H., Mandelkow, E. M. & Mandelkow, E. (1992). The juvenile microtubule-associated protein MAP2c is a rod-like molecule that forms antiparallel dimers. *J. Biol. Chem.* **267**, 10737–10742.
52. Nogales, E., Wolf, S. G. & Downing, K. H. (1998). Structure of the alpha beta tubulin dimer by electron crystallography. *Nature*, **391**, 199–203.
53. Rueda, S., Vicente, M. & Mingorance, J. (2003). Concentration and assembly of the division ring proteins FtsZ, FtsA, and ZipA during the *Escherichia coli* cell cycle. *J. Bacteriol.* **185**, 3344–3351.
54. Lu, C., Stricker, J. & Erickson, H. P. (1998). FtsZ from *Escherichia coli*, *Azotobacter vinelandii*, and *Thermotoga maritima*–quantitation, GTP hydrolysis, and assembly. *Cell Motil. Cytoskeleton*, **40**, 71–86.
55. Sun, Q. & Margolin, W. (1998). FtsZ dynamics during the division cycle of live *Escherichia coli* cells. *J. Bacteriol.* **180**, 2050–2056.
56. Kar, S., Fan, J., Smith, M. J., Goedert, M. & Amos, L. A. (2003). Repeat motifs of tau bind to the insides of microtubules in the absence of taxol. *EMBO J.* **22**, 70–77.
57. Trusca, D., Scott, S., Thompson, C. & Bramhill, D. (1998). Bacterial SOS checkpoint protein SulA inhibits polymerization of purified FtsZ cell division protein. *J. Bacteriol.* **180**, 3946–3953.
58. Miroux, B. & Walker, J. E. (1996). Over-production of proteins in *Escherichia coli*: mutant hosts that allow synthesis of some membrane proteins and globular proteins at high levels. *J. Mol. Biol.* **260**, 289–298.
59. Rivas, G., Lopez, A., Mingorance, J., Ferrandiz, M. J., Zorrilla, S., Minton, A. P., Vicente, M. & Andreu, J. M. (2000). Magnesium-induced linear self-association of the FtsZ bacterial cell division protein monomer. The primary steps for FtsZ assembly. *J. Biol. Chem.* **275**, 11740–11749.
60. Leslie, A. G. W. (1991). Recent changes to the MOSFLM package for processing film and image plate data. *CCP4 and ESF-EACMB Newsletter on Protein Crystallography.* SERC Laboratory, Daresbury, Warrington, UK.
61. Collaborative Computer Project Number 4. (1994). The CCP4 suite: programs for protein crystallography. *Acta Crystallog. sect. D*, **50**, 760–763.
62. Terwilliger, T. C. & Berendzen, J. (1999). Automated MAD and MIR structure solution. *Acta Crystallog. sect. D*, **55**, 849–861.
63. Turk, D. (1992). Weiterentwicklung eines Programms fur Molekulgrafik und Elektronendichte-Manipulation und seine Anwendung auf verschiedene Protein-Strukturaufklarungen. PhD thesis, Technische Universitat Munchen, Germany.
64. Engh, R. A. & Huber, R. (1991). Accurate bond and angle parameters for X-ray protein-structure refinement. *Acta Crystallog.* **47**, 392–400.
65. Schuck, P., Perugini, M. A., Gonzales, N. R., Howlett,

G. J. & Schubert, D. (2002). Size-distribution analysis of proteins by analytical ultracentrifugation: strategies and application to model systems. *Biophys. J.* **82**, 1096–1111.
66. Laue, T. M., Shah, B. D., Ridgeway, T. M. & Pelletier, S. L. (1992). Computer-aided interpretation of analytical sedimentation data for proteins. In *Analytical Ultracentrifugation in Biochemistry and Polymer Science* (Harding, S. E., Rowe, A. J. & Horton, J. C., eds), Royal Society of Chemistry, Cambridge, UK.
67. Kabsch, W. & Sander, C. (1983). Dictionary of protein secondary structure: pattern recognition of hydrogen-bonded and geometrical features. *Biopolymers*, **22**, 2577–2637.
68. Sobott, F., Hernandez, H., McCammon, M. G., Tito, M. A. & Robinson, C. V. (2002). A tandem mass spectrometer for improved transmission and analysis of large macromolecular assemblies. *Anal. Chem.* **74**, 1402–1407.

Edited by R. Huber

(Received 23 October 2003; received in revised form 13 April 2004; accepted 21 May 2004)